



Experimental evaluation of a water spray system for semi-outdoor spaces: Analysis of the effect of the operational parameters

Gianluca Coccia^{a,*}, Serena Summa^a, Elisa Di Giuseppe^b, Marco D'Orazio^b, Michele Zinzi^c, Costanzo Di Perna^a

^a Marche Polytechnic University, Department of Industrial Engineering and Mathematical Sciences (DIISM), Via Brezze Bianche 12, 60131, Ancona, Italy

^b Marche Polytechnic University, Department of Construction, Civil Engineering and Architecture (DICEA), Via Brezze Bianche 12, 60131, Ancona, Italy

^c ENEA, Via Anguillarese 301, 00123, Rome, Italy

ARTICLE INFO

Keywords:

Climate mitigation
Urban overheating
Evaporative cooling
Experimental
Operational parameter

ABSTRACT

As a consequence of climate change, urban overheating has increased in all the cities of the world during the last decades. It is therefore paramount to counteract such effect by promoting the use of effective solutions to mitigate overheating at a micro-scale level. In this work, a modular experimental setup based on a water spray system was designed, realized and tested to evaluate its thermohygrometric performance in semi-outdoor spaces such as bus/train/taxi stops, street resting stations and corner shops. The setup allows to vary three operational parameters: (a) the height of the nozzles from the ground; (b) the presence of an upper shielding to reduce the impact of solar radiation; (c) the presence of a side shielding to reduce the impact of wind speed. The combination of the operational parameters allowed to evaluate the performance of five configurations for the water spray system. Several performance indexes were calculated to assess the impact of each operational parameter. It was found that the best configuration guarantees a -20% reduction of dry-bulb temperature, and the minimum specific water and electricity consumptions of the system are 0.020 L/m^2 and 0.150 Wh/m^2 , respectively. Also, the presence of the side shielding is the parameter that mostly influences the performance of the system, followed by the height of the nozzles, while the presence of the upper shielding has a minor effect. These operational parameters, however, increase relative humidity inside the nebulization volume; it is therefore important to verify if undesired wet conditions are reached.

1. Introduction

There is no doubt that global warming represents a dangerous threat to humanity. The IPCC Sixth Assessment Report [1] highlights that if global warming would reach 1.5°C in the near term (2021–2040), it would be responsible of multiple climate hazards to ecosystems and human beings. The same report evidences that worldwide climate resilient development actions are more urgent than in the past reports, and that immediate and innovative responses may reduce trade-offs between adaptation and mitigation for the sustainable development. Global warming and the phenomenon known as Urban Heat Island (UHI) are strictly correlated [2,3]. Being related to morbidity and mortality caused by heat, the UHI effect represents a serious threat to mankind [4]. Under a research point of view, it is therefore paramount to study and promote innovative solutions to mitigate the UHI effect and urban overheating in a sustainable and effective way.

In order to mitigate UHI and urban overheating, most of literature papers focused on technologies that allow to increase the albedo of

cities and the urban greenery [2,5]. However, in a study carried out by Santamouris et al. [6], different water-based solutions to hinder the UHI effect were evaluated (fountains, pools, ponds, water sprinklers, evaporative wind towers), and it was found that water spraying was the most effective. The working principle of water spray systems is based on the evaporation of water fog that allows to absorb thermal energy from the surrounding air, thus providing an effective cooling solution. This process is somewhat similar to adiabatic humidification, and it is also influenced on the convective phenomena of the fluid in motion. Thus, this technology could be essential to counteract the UHI effect and urban overheating, and to promote outdoor thermal comfort.

As reported in a review paper written by Ulpiani [7], the use of water spray systems witnessed a great diffusion during international exhibitions in cities such as Osaka and Shanghai; additional large installations came next in other cities, such as Seville (for the European Expo in 1992 [8]), Paris [9], Madrid [10]. These installations are part

* Corresponding author.

E-mail addresses: g.coccia@staff.univpm.it (G. Coccia), s.summa@staff.univpm.it (S. Summa), e.digiuseppe@staff.univpm.it (E. Di Giuseppe), m.dorazio@staff.univpm.it (M. D'Orazio), michele.zinzi@enea.it (M. Zinzi), c.diperna@staff.univpm.it (C. Di Perna).

<https://doi.org/10.1016/j.buildenv.2023.110456>

Received 9 January 2023; Received in revised form 9 May 2023; Accepted 25 May 2023

Available online 2 June 2023

0360-1323/© 2023 The Authors. Published by Elsevier Ltd. This is an open access article under the CC BY-NC-ND license (<http://creativecommons.org/licenses/by-nc-nd/4.0/>).

of larger projects, often related to the urban regeneration and with high architectural value, where the thermal migration is only one of the different objectives and, as a consequence, not optimized in terms of comfort improvement and use of resources.

The interest on the technology has received much attention during the last 20 years, and in a recent review Meng et al. [5] noted that more than 50% of the available papers have been published in the last 5 years. These recent studies focused on smaller scale applications with the main objective of improving the thermal comfort conditions; typical applications include pedestrian cool spots, semi-outdoor and temporary spaces, as well as transportation systems [11,12].

Most of studies evaluated solutions for outdoor areas, as they may greatly benefit from evaporative systems even in harsh climates. In 2009, Narumi et al. [13] installed water spray systems on the roof, balcony, and outdoor unit of an air conditioner. The authors used two types of nozzles: one with large water droplets (300 μm size) and one with fine droplets (40 μm size). It was found that the spray system reduced the heat flow by 60% and energy consumption by 80%. In 2010, Wong and Chong [14] installed a water spray system combined with a fan in a high-temperature and high-humidity area (at 1.0 m above the floor level of some outdoor locations of National University of Singapore), and found that air temperature could be reduced by 1.38–1.57 $^{\circ}\text{C}$ and humidity increased by 8.61–10.38%, respectively. In 2011, Huang et al. [15] carried out several experiments in a gazebo and in a waiting area of the Shanghai World Expo Square using a water spray system of 20 nozzles (in transversal arrangement with 400 mm spacing) with nominal pressure of 6 MPa and maximum volume flow rate of the single nozzle of 50 cm^3/min . A temperature drop of 5.0–7.0 $^{\circ}\text{C}$ was registered. The data collected during the experimentation were used to validate a spray cooling model developed to evaluate the cooling performance of the system under different parameters (water pressure: 1.5, 2, 3, 5, 7 MPa; droplet diameter: 16, 26, 40, 60 μm ; airflow rate: 1, 2, 3, 5 m/s ; air temperature: 30 and 38 $^{\circ}\text{C}$; humidity: 40%, 50%, 60%, 70%, 80%) [16]. It was found that droplets of smaller size and lower airflow rates led to a better cooling performance. In 2015, Farnham et al. [17] used a combined system (sprays and fans) to reduce the cooling load of an outdoor area (about 10 m^2) partially shaded by buildings and trees. The nozzles, mounted around the edges of 35 cm fans, could produce droplets with an average diameter of 25 μm . Nominal pressure and volume flow rate were, respectively, 6 MPa and 19 L/h. With this setup, the authors found a temperature drop of 1–2 $^{\circ}\text{C}$. Residents found wet skin moisture acceptable. In the same year, Esen and Tuna [18] evaluated the efficiency of a microfine (5 μm) water spray system coupled with a photovoltaic plant used to reduce its energy consumption. The system was installed in an arbor area (24 m^2) and the authors registered a temperature drop of 20 $^{\circ}\text{C}$, with a humidity increase of about 25%. In 2018, Zheng et al. [19] evaluated the cooling effect of a double-flow pneumatics spray nozzle installed in a climatic chamber. The system worked with 7–9 μm water droplets having a nominal volume flow rate of about 1 L/h at a pressure of 3 bar. Tests were carried out at different combinations of wet bulb depression, pressure and water temperature. The authors found that wet bulb depression is a good indicator to evaluate the operating conditions of the water spray system, while pressure can be varied to achieve optimal cooling at various heights. In 2019, Ulpiani et al. [20] reported the results obtained with two experimental water spray systems installed in two Italian cities (Ancona and Rome). The test rig included 24 hollow-cone nozzles arranged in four parallel strings. The average droplet diameter was 10 μm , while nominal pressure and volume flow rate were, respectively, 70 bar and 1.5 L/min. It was found that temperature could be reduced by 8.2 $^{\circ}\text{C}$, with an increase in relative humidity of 7%. In the same year, some of the authors of the previous study proposed a fuzzy-logic-based control to improve the efficiency of the water spray system and minimize its energy consumption [21]. The implementation of the smart control allowed to reduce air temperature

of 6.14–7.5 $^{\circ}\text{C}$, and to control relative humidity in the range 51.2–67.5%. In 2020, another experimental study was proposed by Ulpiani et al. [22]. In this case, a water spray system including 24 nozzles (mean diameter of 10 μm) was installed on a building roof and results showed that air temperature could be reduced by 7.4 $^{\circ}\text{C}$ at 1.1 m above the ground. In the same year, Desert et al. [23] designed a dynamic gradient spray test station able to produce mist from vertical elements. The nozzles have a cone of 700 mm, and diameters of 0.3 and 0.4 mm were evaluated. The authors demonstrated that air temperature could be lowered by a maximum of 15 $^{\circ}\text{C}$. In addition, no significant increase in relative humidity was found. Oh et al. [24] proposed a combined spray-fan model that was validated experimentally. The system was evaluated according to four operation modes, that include different volume flow rates (240 or 300 cm^3/min) and the presence or not of an air blowing. The nozzles were positioned 3.0 m above the ground. With the fan, the system was able to drop temperature of an additional 3.6 \pm 1.4 $^{\circ}\text{C}$, while humidity increased by 15.9 \pm 4.7%. In 2022, Kim and Kang [25] studied the effect of fog cooling for a system installed in the Daegu Metropolitan City. The authors used a cylindrical-shape spray, positioned 2.7 m from the ground. Three sizes of nozzles (0.15, 0.2, 0.3 mm) were evaluated, with three corresponding values of flow rate (48, 72, 162 cm^3/min). The pressure of the mist was equal to 80 bar. The solution with the fog cooling positioned vertically to the wind direction allowed to reduce the average air temperature by up to 3.02 $^{\circ}\text{C}$. In the same year, Su et al. [26] investigated the cooling performance of a water spray system with different nozzle densities (4, 6, 8 nozzles) and heights (2.3, 2.7, 3.1 m) on pedestrian thermal comfort during summer in Xi'an, China. The area influenced by water mist was equal to 4.5 m^2 . The main results of the study show that the thermohygro-metric performance of the system improved when the number of nozzles increased from 4 to 8, and that the effect of humidification lowered when the height of the nozzles increased from 2.3 to 3.1 m.

The common outcome of the previous studies is that water spray systems create a different micro-climate within the cooled volume delimited by the nozzles' area, which is different and more comfortable in comparison with the surrounding outdoor environment, whatever the urban context might be. Conversely, the cooling potential is very different depending on the system characteristics and boundary conditions; as a matter of fact, temperature reductions vary in the 1.0–9.0 $^{\circ}\text{C}$ range. The previous summary of published papers also hints that, focusing on the thermal performance, there is no common guideline in the design of such systems yet. In addition, Oh et al. [11] highlighted that conventional indexes such as SET* [27], PET [28], WBGT [29] and UTCI [30] are not fully able to represent thermal comfort in a water spray environment, and that more complex models should be considered [11,31–33].

The available experimental works are still limited in number, thus parametric aspects such as the type, number and geometrical distribution of the nozzles used, the configuration of the spray system, the presence of shieldings to reduce the effects of solar radiation and/or wind, and the logic of implemented controls need to be further investigated. The present paper tries to overcome the aforementioned drawbacks by reporting the results of a systematic study conducted with an experimental water spray system designed, realized and tested to evaluate in a quantitative way its thermohygro-metric performance. The case study focuses on a system mainly designed to be used in semi-outdoor spaces such as bus/train/taxi stops, street resting stations and corner shops.

The paper is organized as follows. Section 2 depicts the methodology of the study, and in particular the choice of the configurations and the parameters used to assess their performance. The same section describes the experimental setup and provides detailed information on the components, instruments and sensors used. Section 3 reports the results of the study. Their discussion is provided in Section 4. The main conclusions of the work can be found in Section 5.

Observation period	City	Latitude	Longitude	Altitude (m a.s.l.)	Köppen-Geiger
June - August 2021	Ancona	43.59 N	13.51 E	102	Cfa
	$T_{ext,av}$ (°C)	$RH_{ext,av}$ (%)	$W_{s,av}$ (m/s)	I_{av} (W/m ²)	
	29.9	44	1.6	576	
Month	$T_{ext,max}$	$T_{ext,min}$	$RH_{ext,av}$ (%)	Rainfall (mm)	Heliophany (h)
Jan	9.9	4.7	77	54	5.6
Feb	10.3	4.4	75	56	6.7
Mar	13.3	6.8	75	65	8.4
Apr	16.5	9.9	75	66	10.2
May	21.0	14.3	72	58	11.8
Jun	25.6	18.7	67	40	13.0
Jul	28.4	21.2	63	29	13.0
Aug	28.2	21.3	66	42	11.9
Sep	23.6	17.5	71	62	9.9
Oct	19.4	13.9	77	63	7.5
Nov	15.0	10.0	78	75	6.2
Dec	11.1	6.2	77	71	5.7

Fig. 1. Climatic characterization of the case study location. For the observation period, $T_{ext,av}$ is the average air temperature, $RH_{ext,av}$ is the average relative humidity, $W_{s,av}$ is the average wind speed, and I_{av} is the average global solar radiation incident on the horizontal plane.

2. Materials and methods

To pursue the objective of the study, a supporting structure for the spray system was designed and constructed. It is 6 m long, 4 m wide and 3 m high; all the details are provided in Section 2.2. In accordance with the most recent literature, the size was selected to host a misting system suitable for small scale, semi-outdoor applications to be used as cooling shelters, such as: street resting station, corner shop, gazebo, bus/train/taxi waiting shelter. The structure is modular and easy replicable, and its dimensions make it suitable for the aforementioned settings. In this sense, the system represents a realistic installation, which might be adapted to specific architectural and design needs but maintaining its technological features.

The structure was conceived to allow different operational settings and the water spray system was evaluated as a function of the following conditions: (a) height of the nozzles with respect to the ground (2.20, 2.60 or 2.90 m); (b) presence or absence of the upper shielding cloth to reduce the influence of solar radiation; (c) presence or absence of the side shielding cloth to reduce the influence of wind. The performance of the system is assessed by comparing the micro-climatic conditions within the structure against those monitored in the surrounding undisturbed area. The experimental campaign was started in the second half of June 2021 and carried out until the end of August 2021. The water spray system was activated at 09:00 am and kept on until 19:00 pm; it could be also automatically deactivated when the outdoor temperature was lower than 26 °C, or when rain began.

Being an experimental study, some limitations applies. The focus is on a given object in given climatic conditions; this implies that important information on the impact of operational settings on the performance of the spray system can be derived. Conversely, no general design criteria and guideline can be implemented because of the many variables involved in the process, especially the climatic ones which severely affect the performance of the system.

2.1. Case study location

Fig. 1 reports the main climatic information of the location chosen for the experimentation. The experimental setup was installed in an outdoor space near the Faculty of Engineering of Marche Polytechnic University, Ancona, Italy (Fig. 2). In Fig. 1, the geographic coordinates are provided together with the Köppen–Geiger climate classification [34]. Ancona is a coastal city, thus presenting mild and temperate Mediterranean climatic conditions.

2.2. Experimental setup: design and installation

The experimental setup has a modular and flexible design, used to test the water spray system under different operational configurations. The structure used to support the nozzles is realized with profiles made of aluminum. The structure is anchored to the ground by means of tie-beams, in order to make it stable and wind-resistant; it occupies an area A_{ws} of around 24 m² (4 m x 6 m) and it is 3-m high respect to the ground (Figs. 3 and 4). Eight aluminum profiles, 2-m long, are installed in the main structure and they can be fixed at different heights from the ground in order to vary the vertical position of the nozzles. Four pipes including the nozzles are disposed parallel to the longer side of the structure, using the support of four steel cables inserted into rings provided in the grooves of the aluminum profiles. In this way, there is the possibility to vary the wheelbase of the pipes. In the main structure, it is also possible to install two shielding cloths: (a) an upper shielding used to mitigate the effect of solar radiation; and (b) a 4-side shielding used to mitigate the effect of wind speed.

The cooling system consists of a pump, the nozzles and the hydraulic circuit. The pump is an axial Premium 70-bar, 3 l/min, 230 V 50 Hz model, which includes a manometer, inlet and outlet valves, and a pressure switch to avoid unintentional dry-running. A filter is installed upstream of the pump, while from the main 1/4" polyamide pipe four branches are derived (a branch for each pipe that includes the nozzles). Each pipe is equipped with six nozzles, for a total of 24 nozzles. The nozzles, made of stainless-steel, are type 0.20 mm 10/24" with body in nickel-plated brass and anti-drop system. The cooling system includes other sensors connected to the pump: a rain sensor, able to turn the pump off in case of rain; a turbine flow-meter, used to measure the instantaneous volume flow rate and determine the amount of consumed water; an electrical energy meter, to evaluate the electricity consumption of the pump.

In order to reduce the consumption of electrical energy and to make the water spray system as independent as possible from the power grid, a photovoltaic system is installed near the nebulization structure and used to power the pump of the cooling system (Fig. 4). The photovoltaic system includes 4 panels with PERC-type monocrystalline silicon cells (DXM6-60P/BF, Sun–Earth). Each panel has a nominal electrical power of 300 W and an useful surface of 1.63 m². The panels, South-facing, are inclined of 20° with respect to the ground to maximize energy production during the summer season. The inverter (model EDISON3024) is a pure sine wave device with an integrated PWM charge controller that is used to manage an electrical storage of 4 AGM-deep cycle batteries with a nominal overall capacity of 7200 Wh. When the electrical storage is not able to provide energy, the inverter can power the pump by drawing power directly from the grid.



Fig. 2. Outdoor space used for the experimental campaign.

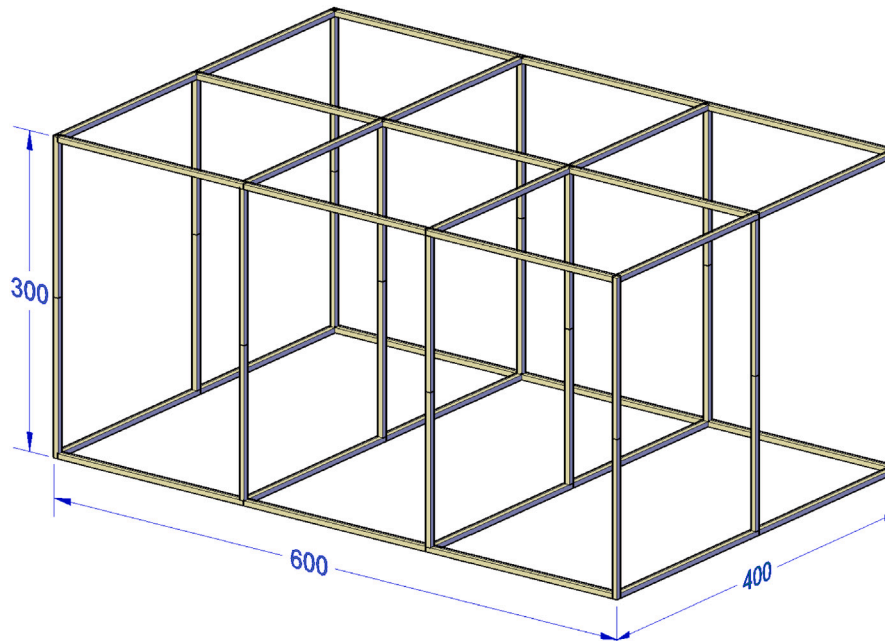


Fig. 3. Aluminum support structure (lengths in cm).

Several sensors are installed inside and outside the structure housing the water spray system to evaluate its operation and performance (Table 1 and Fig. 5). The outdoor conditions are measured by means of a meteorological station installed near the water spray system. The station includes the temperature, humidity, wind and solar radiation sensors described in Table 1. The structure housing the water spray system is instead equipped with temperature and humidity sensors. Four PCMINI sensors (Michell Instruments) are used to measure both dry-bulb temperature and relative humidity, and are mounted on a stand that allows to vary their height from the ground (the height was kept fixed at 1.10 m). The sensors are shielded in order to reduce the effect of solar radiation. Two globe-thermometers based on Pt100 are also installed inside the water spray system to evaluate the radiant mean temperature. The globes were installed at a fixed height from the ground of 1.80 m.

The acquisition of all measurement data, along with the control of the water spray system, is managed with the software LabVIEW by National Instruments, installed in a desktop computer located in a cabin near the nebulization system.

2.3. Identification of the performance indicators

The variation of one or more operational parameters allowed to define five different configurations for the water spray system. The details of each configuration are provided in Table 2 and their thermal performance was evaluated based on the difference between the average dry-bulb temperature detected by the four temperature sensors inside the nebulization structure ($T_{ws,av}$) and the outdoor dry-bulb temperature detected by the meteorological station (T_{ext}), difference

Table 1
Sensors used in the experimental setup.

Measure	Sensor type	Model	Range	Accuracy
Meteorological station				
Air temperature	Thermo hygrometer (Pt100)	DMA 875	-30–70 °C	±0.2 °C
Relative humidity	Thermo hygrometer (Capacitive hygrometer)	DMA 876	0–100%	1.5%
Wind velocity	Tacogonioanemometer (Cup type)	DNA 022	0–60 m/s	1.5%
Wind direction	Tacogonioanemometer (Cup type)	DNA 022	0–360°	1.0%
Horiz. solar radiation	Global radiometer	SR30-M2-D1	0–4000 W/m ²	3.0%
Diffuse solar radiation	Global radiometer + shadow band	DPA 153 + DPA245	0–2000 W/m ²	5.0%
Experimental setup				
Air temperature	Thermo hygrometer (Pt100)	PCMINI52	-20–80 °C	±0.2 °C
Relative humidity	Thermo hygrometer (Capacitive hygrometer)	PCMINI53	0–100%	±2%
Mean radiant temperature	Globe temperature sensor (Pt100)	EST131	-30–70 °C	±0.15 °C
Air temperature	Thermocouple (T type)	-	-220–400 °C	-

Table 2
Configurations of the water spray system and average outdoor conditions.

Conf.	Nozzles h. (m)	Upper shield.	Side shield.	T _{ext,av} (°C)	RH _{ext,av} (%)	W _{s,av} (m/s)	I _{max} (W/m ²)	I _{d,av} (W/m ²)
1	2.60	No	No	31.6	42	1.9	1098	257
2	2.60	Yes	No	27.5	48	1.7	1141	177
3	2.20	Yes	No	27.7	46	1.7	910	149
4	2.20	Yes	Yes	29.6	51	1.5	1004	211
5	2.90	Yes	Yes	31.0	41	1.3	1178	355



Fig. 4. Support structure equipped with the cooling system, the sensors and part of the 4-side shielding cloth.

that was related to the outdoor temperature itself:

$$\epsilon_T = \frac{T_{ws,av} - T_{ext}}{T_{ext}} = \frac{\Delta T}{T_{ext}} \quad (1)$$

In a same fashion, the humidity variation due to water nebulization was evaluated based on the difference between the average relative

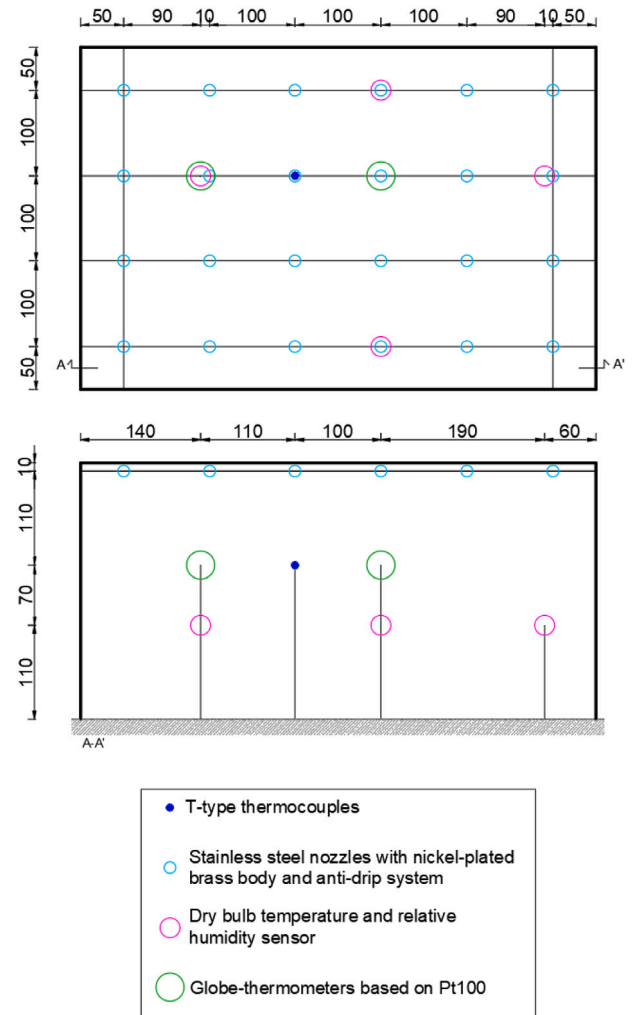


Fig. 5. Top view and side view of the cooling system (lengths in cm).

humidity detected by the four humidity sensors inside the nebulization structure ($RH_{ws,av}$) and the outdoor relative humidity detected by the meteorological station (RH_{ext}), difference related to the outdoor relative humidity:

$$\epsilon_{RH} = \frac{RH_{ws,av} - RH_{ext}}{RH_{ext}} = \frac{\Delta RH}{RH_{ext}} \quad (2)$$

An additional indicator defined $MOCI$ (Mediterranean Outdoor Comfort Index) was evaluated to establish the degree of thermohygrometric comfort provided by the water spray system. $MOCI$ was developed based on an extended statistical survey [35] and is a dimensionless index based on the ASHRAE (American Society of Heating, Refrigerating and Air-Conditioning Engineers) 7-point scale ($-3 =$ “cold”; $-2 =$ “cool”; $-1 =$ “slightly cool”; $0 =$ “neutral”; $+1 =$ “slightly warm”; $+2 =$ “warm”; $+3 =$ “hot”) [36]. In the same fashion of the PMV index [37], thermohygrometric comfort conditions can be assessed when $MOCI$ falls in the range between -0.5 and 0.5 . Inside the water spray system, $MOCI_{ws}$ can be evaluated as follows:

$$MOCI_{ws} = -4.257 + 0.325 I_{cl,ws} + 0.146 T_{ws,av} + 0.005 RH_{ws,av} + 0.001 I - 0.235 W_s \quad (3)$$

where I is the global solar radiation incident on the horizontal plane (W/m^2), W_s is the wind speed (m/s) and $I_{cl,ws}$ is the thermal clothing insulation (clo), defined as function of the air temperature inside the nebulization system [35]:

$$I_{cl,ws} = 1.608 - 0.038 T_{ws,av} \quad (4)$$

The $MOCI$ index was also used to evaluate thermohygrometric comfort outside the nebulization system; in this case:

$$MOCI_{ext} = -4.257 + 0.325 I_{cl,ext} + 0.146 T_{ext} + 0.005 RH_{ext} + 0.001 I - 0.235 W_s \quad (5)$$

where $I_{cl,ext}$ was evaluated as:

$$I_{cl,ext} = 1.608 - 0.038 T_{ext} \quad (6)$$

It is therefore possible to define for each configuration the difference between the two previous $MOCI$ indexes as:

$$\Delta MOCI = MOCI_{ws} - MOCI_{ext} \quad (7)$$

The delta difference $\Delta MOCI$ can be used to define two additional performance parameters of the water spray system referred to the unit surface area of the installation (A_{ws} , equal to $24 m^2$ for the nebulization system under study). The first parameter, S_w (L/m^2), takes into account the water consumption of the system, and can be expressed as follows:

$$S_w = \frac{C_w}{A_{ws} \frac{1}{n} \sum_{i=1}^n |\Delta MOCI_i|} \quad (8)$$

where n is the number of evaluation points for each configuration and C_w is the overall water consumption of the system (L) for each configuration. In a similar fashion, the second performance parameter, S_e (Wh/m^2), refers to the electricity consumption of the system and is evaluated as:

$$S_e = \frac{C_e}{A_{ws} \frac{1}{n} \sum_{i=1}^n |\Delta MOCI_i|} \quad (9)$$

where C_e is the overall electrical energy consumption of the system (Wh) for each configuration. The two specific consumption indexes S_w and S_e can be regarded as two figures of merit that can be used to assess and compare the efficiency (respectively in terms of water and electrical energy used) of different water spray systems.

3. Results of the experimental campaign

In this section, the experimental results obtained for each of the five configurations defined in Section 2.3 will be reported and discussed. Each configuration will be analyzed separately, and a comparison between configurations where only an operational parameter was being varied will be examined. The analysis ends with a

summary performance evaluation of the water spray system for each configuration.

3.1. Results for the different configurations

This section discusses the experimental results collected for each examined configuration of the water spray system.

3.1.1. Configuration 1

Configuration 1 was set with the following operational parameters (Table 2): (a) height of the nozzles of 2.60 m with respect to the ground; (b) no upper shielding to reduce the influence of solar radiation; (c) no side shielding to reduce the influence of wind.

Fig. 6(a) shows how the delta difference ΔT between the average temperature detected inside the water spray system and the outdoor temperature T_{ext} varies with the outdoor temperature itself. It can be seen that ΔT lowers for higher values of T_{ext} . This trend is confirmed by numerical simulations [38,39] and highlights that the water spray system improves its performance with higher external temperatures. Fig. 6(b) plots the term ΔRH vs. T_{ext} . In this case, there is an opposite trend that is always confirmed by numerical analysis [38,39]: at higher outdoor temperatures, the nebulization system reacts with a greater production of water vapor that lowers perceived temperature inside the structure. The indexes $MOCI_{ws}$ and $MOCI_{ext}$ are plotted in Fig. 6(c). It can be observed that the perceived thermal sensation inside the water spray system is always better with respect to outside, even if the internal environment remains “slightly warm”.

3.1.2. Configuration 2

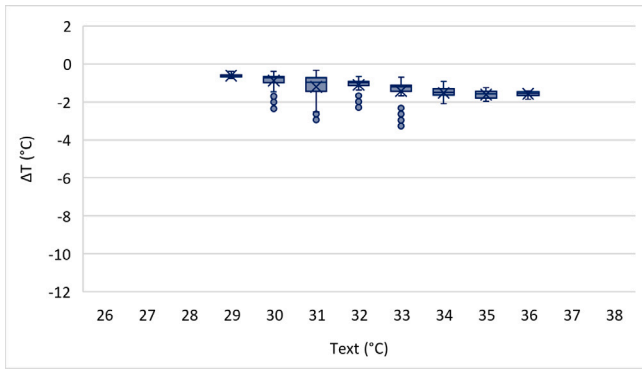
Configuration 2 was set with the following operational parameters (Table 2): (a) height of the nozzles of 2.60 m with respect to the ground; (b) upper shielding to reduce the influence of solar radiation; (c) no side shielding to reduce the influence of wind. The only operational parameter that differs with respect to configuration 1 is (b), the presence of the upper shielding.

Based on Fig. 7(a), it is clear that the water spray system is able to reduce the air temperature perceived inside the nebulization volume. With respect to configuration 1 it can be noted that, for similar outdoor temperatures, ΔT is greater. This effect is likely due to the presence of the upper shielding, which reduces the impact of solar radiation inside the nebulization system. The influence of the upper shielding is also visible in Fig. 7(c), where it is evident that the perceived thermal comfort inside the nebulization volume is significantly better with respect to the outdoor environment (“slightly warm” or “slightly cool”). It is important to note that in this configuration (and in the other configurations that use the upper shielding) $MOCI_{ws}$ (Eq. (3)) was evaluated with the value of diffuse solar radiation incident on the horizontal plane (I_d). This choice is more consistent with the presence of the upper shielding in the water spray system, and also allowed to obtain more realistic values for $MOCI_{ws}$.

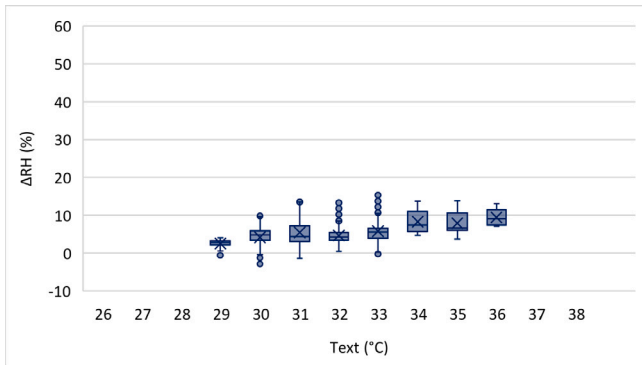
3.1.3. Configuration 3

Configuration 3 was set with the following operational parameters (Table 2): (a) height of the nozzles of 2.20 m with respect to the ground; (b) upper shielding to reduce the influence of solar radiation; (c) no side shielding to reduce the influence of wind. The only operational parameter that differs with respect to configuration 2 is (a), the height of the nozzles.

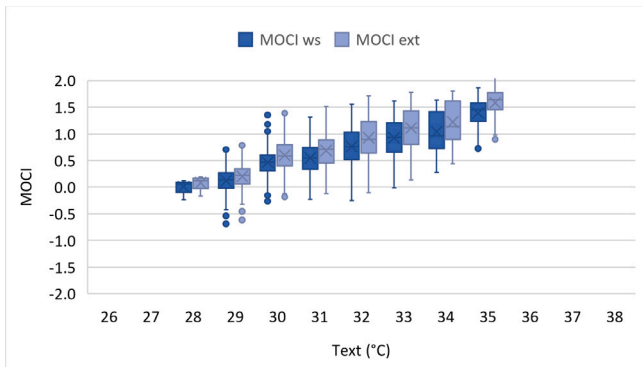
The trends for ΔT and ΔRH discussed for the previous configurations are confirmed for configuration 3, too (Figs. 8(a) and 8(b)). A direct comparison with configuration 2 reveals that, for equal external temperatures, configuration 3 is able to guarantee a better performance under the thermal point of view, but also a greater production of water vapor. This behavior is due to the lower height of the nozzles, which is 40 cm nearer the ground with respect to configuration 2. The performance of the examined system is also visible in Fig. 8(c), which shows that $\Delta MOCI$ is greater than configuration 2 for the same external temperatures. The thermal sensation is generally “slightly cool”.



(a) Dry-bulb temperature difference between the water spray system and the outdoor.

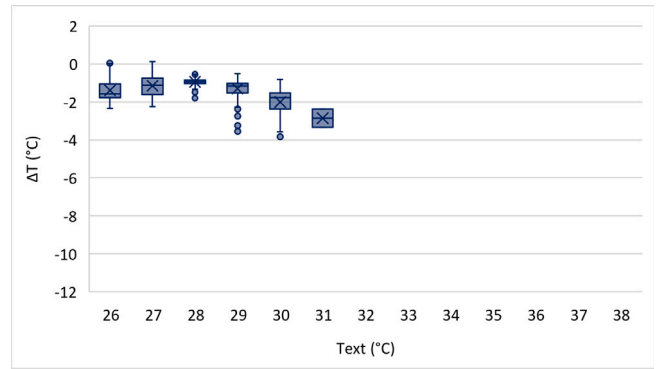


(b) Humidity difference between the water spray system and the outdoor.

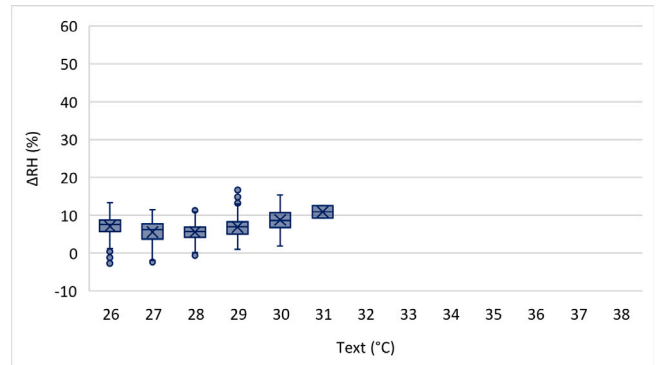


(c) *MOCI* indexes.

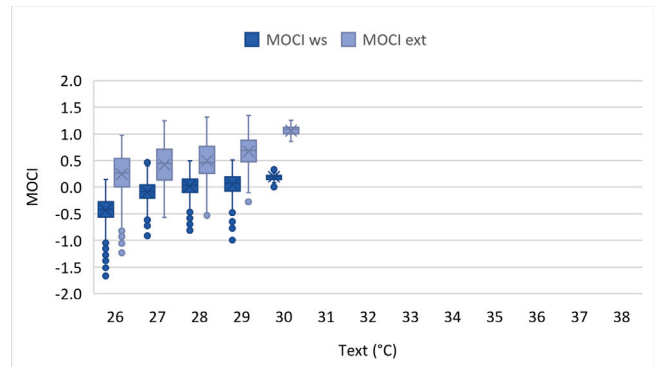
Fig. 6. Thermohygro-metric performance of configuration 1 as function of the outdoor temperature.



(a) Dry-bulb temperature difference between the water spray system and the outdoor.



(b) Humidity difference between the water spray system and the outdoor.



(c) *MOCI* indexes.

Fig. 7. Thermohygro-metric performance of configuration 2 as function of the outdoor temperature.

3.1.4. Configuration 4

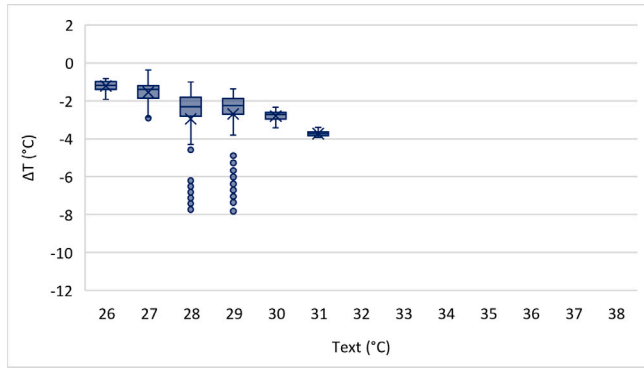
Configuration 4 was set with the following operational parameters (Table 2): (a) height of the nozzles of 2.20 m with respect to the ground; (b) upper shielding to reduce the influence of solar radiation; (c) side shielding to reduce the influence of wind. The only operational parameter that differs with respect to configuration 3 is (c), the presence of the side shielding.

Fig. 9(a) clearly shows that the combined presence of the upper and side shielding, together with a low height of the nozzles, results in a dramatic thermal improvement of the water spray system, especially at higher external temperatures. However, the containment of the structure limits the exchange with external air, thus resulting in

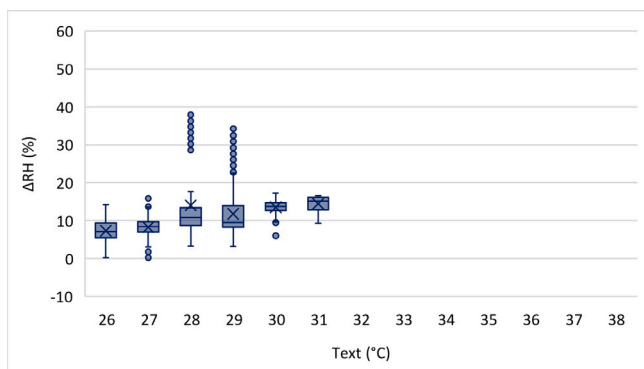
a remarkable increasing of relative humidity inside the nebulization volume (Fig. 9(b)). The thermohygro-metric sensation expected inside the water spray system for configuration 4 is plotted in Fig. 9(c), where it is clear that the perceived thermal comfort results in a general better condition with respect to configuration 3. The reason may lie in the fact that the *MOCI* index is less sensible to relative humidity with respect to other thermohygro-metric parameters.

3.1.5. Configuration 5

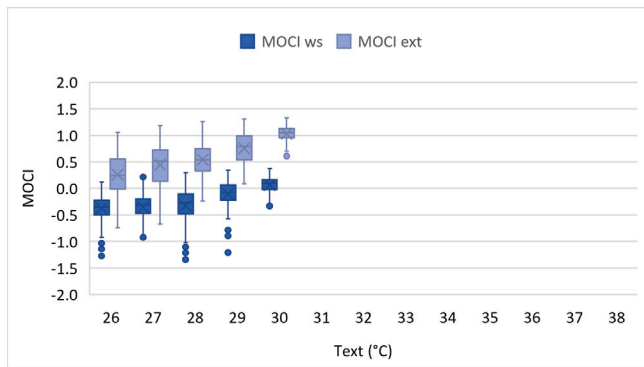
Configuration 5 was set with the following operational parameters (Table 2): (a) height of the nozzles of 2.90 m with respect to the ground; (b) upper shielding to reduce the influence of solar radiation;



(a) Dry-bulb temperature difference between the water spray system and the outdoor.



(b) Humidity difference between the water spray system and the outdoor.

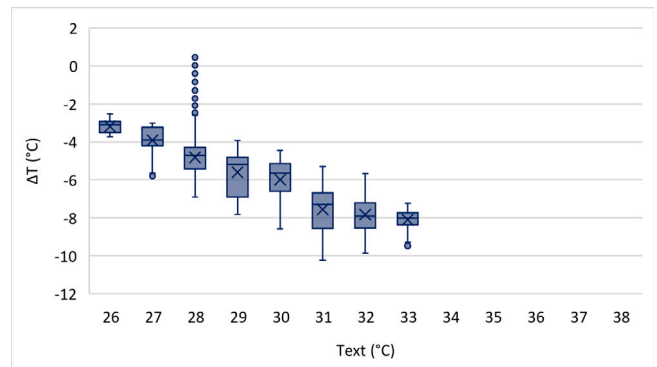


(c) MOCI indexes.

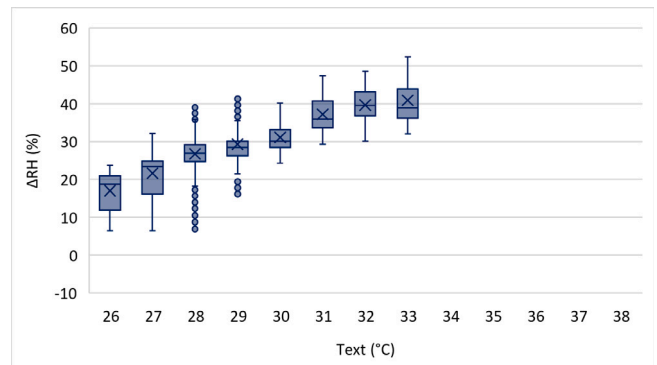
Fig. 8. Thermohygrometric performance of configuration 3 as function of the outdoor temperature.

(c) side shielding to reduce the influence of wind. The only operational parameter that differs with respect to configuration 4 is (a), the height of the nozzles.

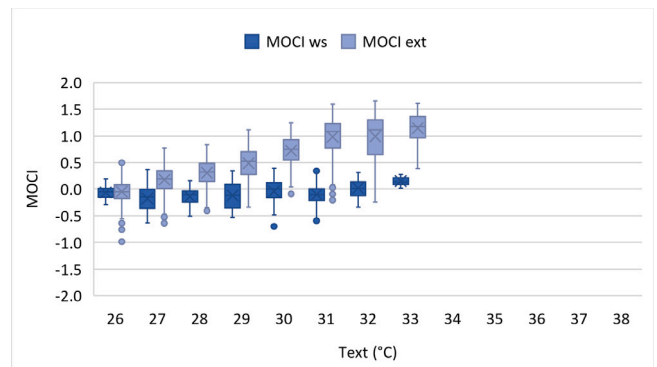
In this case, the higher height of the nozzles worsens the thermal performance of the water spray system (Figs. 10(a) and 10(b)); however, the behavior of the system is similar to that found for configuration 4. The index $MOCI_{ws}$ inside the nebulization volume is more variable with configuration 5, with a typical “slightly warm” sensation (Fig. 10(c)).



(a) Dry-bulb temperature difference between the water spray system and the outdoor.



(b) Humidity difference between the water spray system and the outdoor.

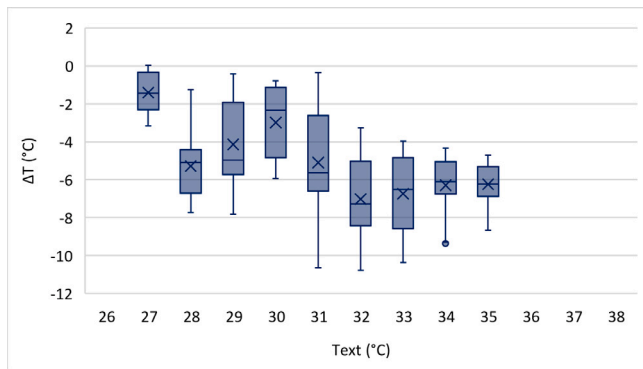


(c) MOCI indexes.

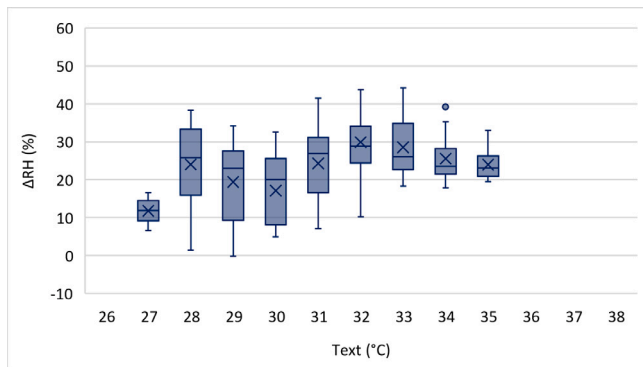
Fig. 9. Thermohygrometric performance of configuration 4 as function of the outdoor temperature.

3.2. Summary of the results

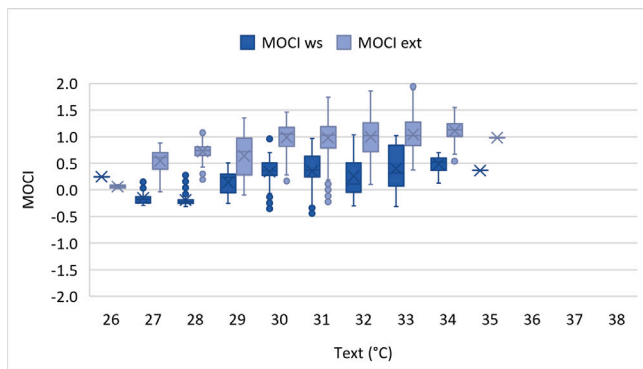
Considering all the experimental points collected for the five configurations of the water spray system, it is possible to evaluate the performance parameters ϵ_T and ϵ_{RH} as defined in Section 2.3. Figs. 11 and 12 show the values of the two parameters for each configuration. From the first figure, it can be noted that the water spray system is always able to reduce the perceived air temperature. The best configuration is 4, which guarantees an average -20% reduction of air temperature thanks to a combination of low height of the nozzles, presence of the upper shielding and presence of the side shielding. This



(a) Dry-bulb temperature difference between the water spray system and the outdoor.



(b) Humidity difference between the water spray system and the outdoor.



(c) *MOCI* indexes.

Fig. 10. Thermohygro-metric performance of configuration 5 as function of the outdoor temperature.

remarkable reduction, however, is accompanied by a relevant production of water vapor, as it is clear from Fig. 12 (+69%). Configuration 5, with the maximum height of the nozzles, performs not so differently from configuration 4, both in terms of air temperature (−17%) and humidity (+64%). Configuration 1 and 2 are not able to reach an average air temperature reduction of −5%. Configuration 3, instead, is able to reach a −8% temperature reduction and ensures an acceptable increase of water vapor production (+27%).

Fig. 13 depicts the values of $\Delta MOCI$ obtained for each configuration. It is possible to note that configuration 1 is not able to improve *MOCI* considerably. The remaining configurations, instead, allow to reach a $\Delta MOCI$ lower than −0.5, with the best average performance

obtained by configuration 3 (−0.79). For this last configuration, Fig. 14 shows how $\Delta MOCI$ varies with ΔT . The growing trend confirms that the perceived thermal sensation inside the water spray system improves when the air internal temperature is cooler than outside. In the same fashion, Fig. 15 depicts that the perceived thermal sensation inside the nebulization system improves when there is a larger production of water vapor.

The specific consumption indexes S_w and S_e for each configuration are provided in Fig. 16. In Eqs. (8) and (9), the consumption values C_w and C_e are based on the readings of the sensors installed in the experimental setup (Section 2.2). Since the volumetric flow rate of water is about 100 L/h while the electrical absorption of the pump is equal to about 740 W, in a typical day with the water spray system working from 09:00 am to 19:00 pm, the average overall consumptions are 1000 L and 7400 Wh, respectively. As regards the specific consumption of water, S_w , it is possible to note that the worst configuration is 1 (0.098 L/m²), where there is no upper/side shielding. The remaining configurations, instead, have similar water consumption indexes, with the minimum reached by configuration 3 (0.020 L/m²). The specific electricity consumption index, S_e , has a similar trend for the five configurations. In this case, the less efficient solution is again configuration 1, with a specific consumption of 0.725 Wh/m². The other solutions are much more efficient, with the minimum consumption still obtained by configuration 3 (0.150 Wh/m²).

4. Discussion

Based on the results obtained with the experimental analysis, it is clear that substantial improvements in the perceived thermohygro-metric sensation can be obtained only with a combination of reduced height of the nozzles and presence of at least one shielding (upper or side). With configuration 1, which does not provide any shielding (Table 2), most of the water mist is in fact not able to reach the volume occupied by pedestrians, because the mist is dispersed by the action of wind. This dispersion also worsens the water and electricity consumptions of the system (Fig. 16). From Fig. 11, it is evident that the simple addition of the upper shielding (configuration 2) is not sufficient to improve significantly the thermal performance of the water spray system, because the effect of solar radiation on the perceived thermal sensation is limited. Configuration 3, which reduces the height of the nozzles with respect to the previous configurations (from 2.60 to 2.20 m), leads to a better performance, because the mist is able to interact with the air inside the nebulization system for a longer period. The best thermal performance is achieved by configuration 4, because with this solution there is the combination of a low height of the nozzles and the presence of both the shieldings. The effect of the side shielding is particularly evident in Figs. 11 and 12 when compared to configuration 3: with the side shielding, the circulation of air inside the water spray system is limited, thus renovation of drier but hotter air by the action of wind is effectively counteracted. Configuration 5 and 4 only differ for the height of the nozzles (2.90 and 2.20 m, respectively). With a greater distance from the ground, the nozzles evaluated with configuration 5 are not able to provide the same thermal performance of the previous configuration. Based on preliminary tests conducted by the authors, the 2.20 m configurations should not result in a disturbing wet sensation to human beings. For this reason, configuration 5 is not recommended against configuration 4.

Among the three operational parameters evaluated in the present study, the quantity that mostly influences the performance of the water spray system is the side shielding. The height of the nozzles shows a minor effect, while the presence of the upper shielding has a limited influence on the performance of the system. As seen through the experimental analysis, however, the first two operational parameters can have a great impact on the increase of relative humidity inside the nebulization volume (Fig. 12). Thus, it is important to carefully check if undesired humidity and wet conditions are reached by pedestrians.

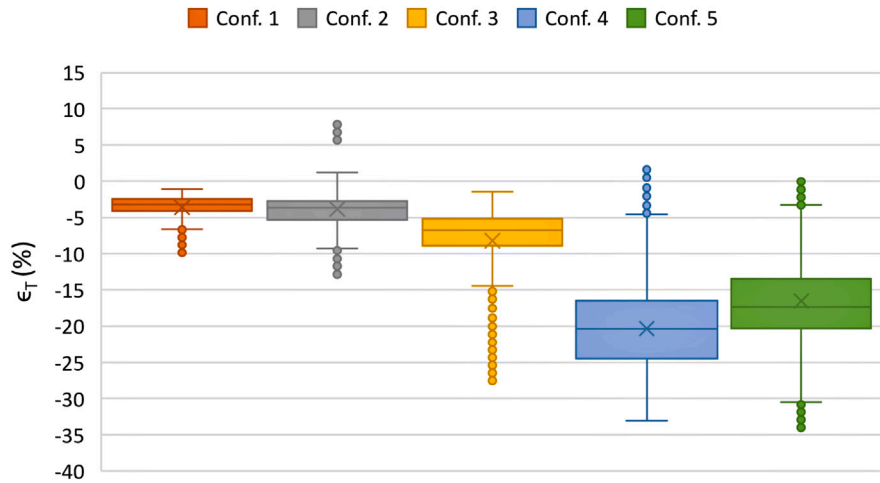


Fig. 11. Relative dry-bulb temperature difference between the water spray system and the outdoor for each configuration.

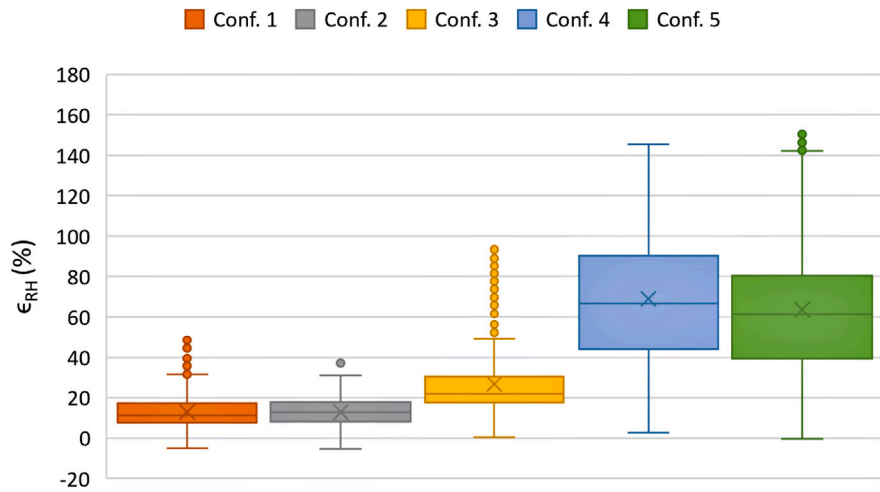


Fig. 12. Relative humidity difference between the water spray system and the outdoor for each configuration.

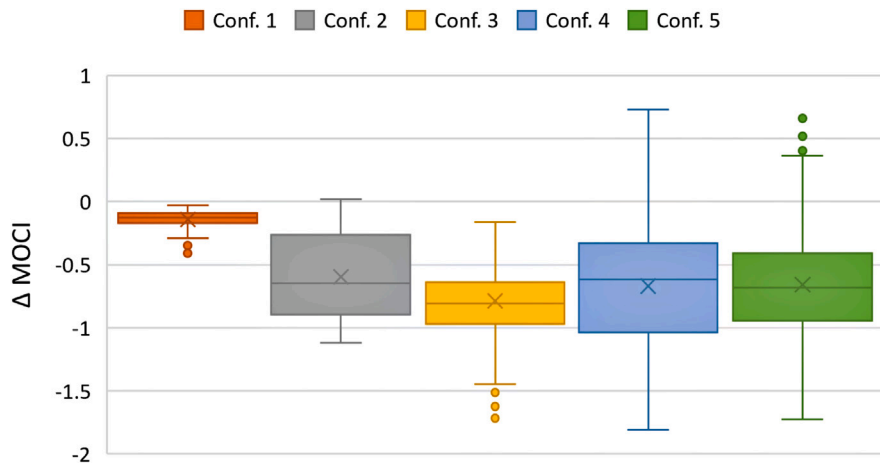


Fig. 13. Difference of the MOCI indexes evaluated inside and outside the water spray system for each configuration.

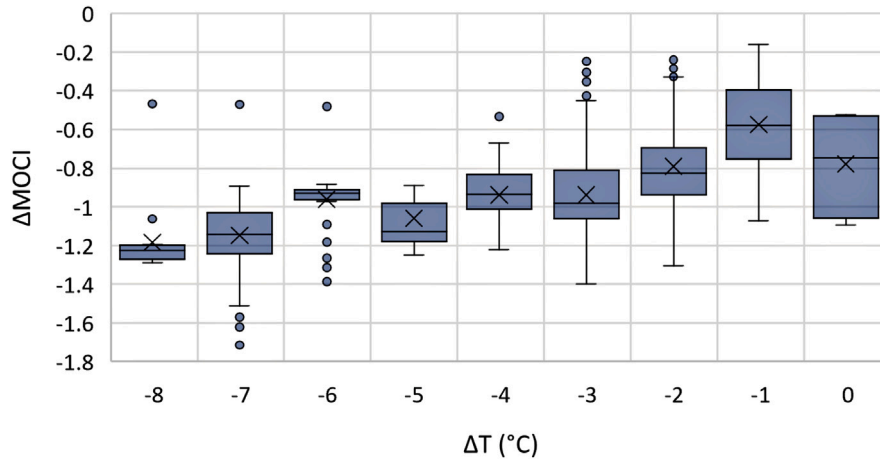


Fig. 14. Difference of the *MOCI* index evaluated inside and outside the water spray system for configuration 3 at various dry-bulb temperature differences.

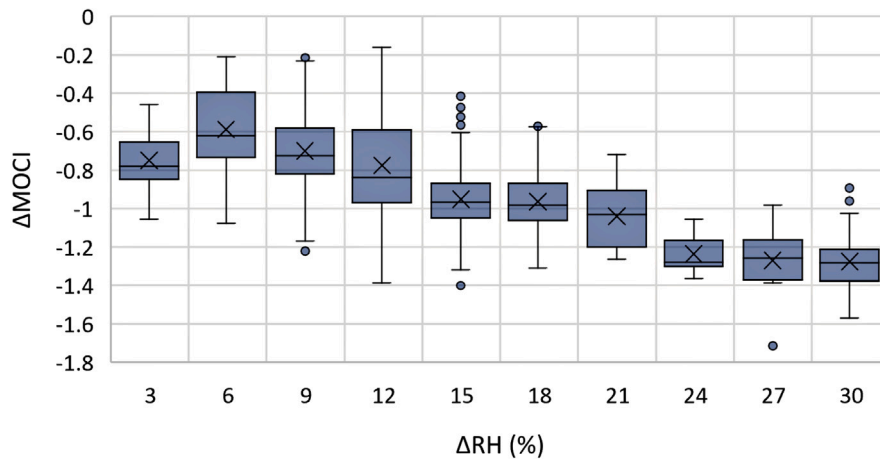


Fig. 15. Difference of the *MOCI* index evaluated inside and outside the water spray system for configuration 3 at various relative humidity differences.

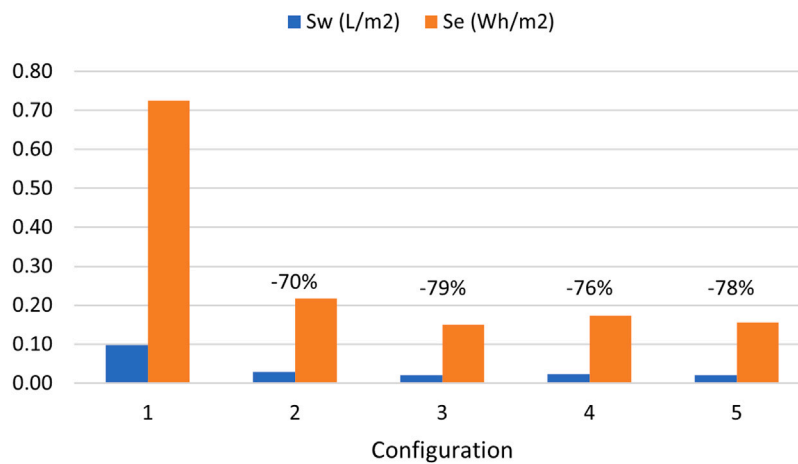


Fig. 16. Specific consumptions indexes for each configuration. The percentage variations are referred to configuration 1.

This aspect will be examined in more detail in a future study. Based on the previous considerations, the solution that guarantees an adequate compromise between evaporative cooling effect, limited humidity increase and acceptable water/electricity consumption is therefore configuration 3.

The water spray system described in the present work was characterized carrying out several measurements that allowed to evaluate different working conditions. It should be noted, however, that such working conditions can vary with time and according to the point considered inside the water system, because possible installations can refer to gazebos, streets, etc. Thus, there cannot be a generic representativity for the water spray system under study. In any case, experimental measurements such as those proposed can be used to validate numerical models, so even the non-specific representativity of the system can be useful, as also demonstrated by previous works of the authors [20–22].

Another aspect that should be considered is that water spray systems are spreading rapidly and without a real awareness of their correct utilization (e.g. they are often used in conditions of high windiness or low outdoor temperatures). This aspect is paramount as means increased consumption of water and electrical energy. For this reason, further studies in real environments are required, also considering that the existing literature is far from being comprehensive on the topic.

5. Conclusions

This study discussed the design, realization and testing of a modular water spray system used to improve thermal comfort in semi-outdoor urban spaces. The thermohygro-metric performance of the system was experimentally evaluated based on five configurations that differ in three operational parameters: (a) height of the nozzles from the ground (2.20, 2.60 or 2.90 m); (b) presence or absence of an upper shielding to mitigate the influence of solar radiation; (c) presence or absence of a 4-side shielding to mitigate the influence of wind. Based on the results of the study, the following key considerations can be drawn.

- All the configurations evaluated in the present paper allow to lower the dry-bulb air temperature, but the solution that guarantees an adequate degree of evaporative cooling and an acceptable increase of humidity is configuration 3. This configuration uses nozzles at their lowest height (2.20 m), an upper shielding for solar radiation, and no side shielding to reduce the effect of wind speed. In average, configuration 3 is able to reduce the dry-bulb air temperature of -8% and guarantees the lowest values of S_w and S_e . However, even if the $MOCI_{ws}$ index for this solution is adequate (“slightly cool” thermal sensation), further experimentations are required to assess the real comfort conditions of human beings, especially when it comes to humidity and wet sensations. Based on preliminary tests conducted by the authors, the 2.20 m configurations should not result in a disturbing wet sensation to human beings.
- The operational parameter that mostly influences the performance of the water spray system is the presence of the side shielding. The side shielding, however, limits the air circulation inside the nebulization system and this noticeably increases the rate of relative humidity in the volume occupied by pedestrians. It is therefore important to check if undesired humidity or wet conditions are registered by people. In general, the configurations that use the side shielding assure the best thermal performance of the nebulization system (configurations 4 and 5). The same configurations also present low values of S_w and S_e .
- The upper shielding used to reduce the effect of solar radiation seems to have a limited influence on the performance of the water spray system, while the height of the nozzles shows a greater effectiveness. In this last case, however, humidity and wet conditions should be carefully checked for the lower heights. This aspect will be examined in more detail in a future study.

Nomenclature

Latin Symbols

A	Surface area (m^2)
C	Consumption (L or Wh)
I	Global incident solar radiation on the horizontal plane (W/m^2)
I_{cl}	Thermal clothing insulation (clo)
$MOCI$	Mediterranean Outdoor Comfort Index
n	Number of evaluation points
PMV	Predicted Mean Vote
RH	Relative humidity (%)
S	Specific consumption index (L/m^2 or Wh/m^2)
T	Temperature ($^{\circ}C$)
W_s	Wind speed (m/s)

Greek Symbols

Δ	Delta difference
ϵ	Relative difference (temperature or relative humidity) (%)

Subscripts

av	Average
d	Diffuse
e	Electrical
ext	External
h	Heating
max	Maximum
ref	Reference
w	Water
ws	Water spray

Acronyms

AGM	Absorbent Glass Mat
ASHRAE	American Society of Heating, Refrigerating and Air-Conditioning Engineers
IPCC	Intergovernmental Panel on Climate Change
PERC	Passivated Emitter and Rear Cell
PWM	Pulse Width Modulation
PET	Physiological Equivalent Temperature
SET*	Standard Effective Temperature
UHI	Urban Heat Island
UTCI	Universal Thermal Climate Index
WBGT	Wet-Bulb Globe Temperature

CRedit authorship contribution statement

Gianluca Coccia: Writing – original draft, Methodology, Investigation, Conceptualization. **Serena Summa:** Validation, Methodology, Investigation, Data curation. **Elisa Di Giuseppe:** Writing – review & editing, Methodology. **Marco D’Orazio:** Writing – review & editing, Methodology. **Michele Zinzi:** Writing – review & editing, Methodology, Funding acquisition. **Costanzo Di Perna:** Supervision, Project administration, Methodology, Funding acquisition.

Declaration of competing interest

The authors declare that they have no known competing financial interests or personal relationships that could have appeared to influence the work reported in this paper.

Data availability

Data will be made available on request.

Acknowledgments

Funding: This work was supported by the Italian Ministry of Economic Development under the framework program “Research of the Electricity System”.

References

- [1] Working Group II, IPCC Sixth Assessment Report, 2022.
- [2] M.J. Alcoforado, H. Andrade, Global Warming and the Urban Heat Island, 2008, pp. 249–262.
- [3] M. Santamouris, On the energy impact of urban heat island and global warming on buildings, *Energy Build.* 82 (2014) 100–113.
- [4] J. Wang, S. Liu, Z. Liu, X. Meng, C. Xu, W. Gao, An experimental comparison on regional thermal environment of the high-density enclosed building groups with retro-reflective and high-reflective coatings, *Energy Build.* (2022).
- [5] X. Meng, L. Meng, Y. Gao, H. Li, A comprehensive review on the spray cooling system employed to improve the summer thermal environment: Application efficiency, impact factors, and performance improvement, *Build. Environ.* (2022) 109065.
- [6] M. Santamouris, L. Ding, F. Fiorito, P. Oldfield, P. Osmond, R. Paolini, D. Prasad, A. Synnefa, Passive and active cooling for the outdoor built environment - Analysis and assessment of the cooling potential of mitigation technologies using performance data from 220 large scale projects, *Sol. Energy* 154 (2017) 14–33.
- [7] G. Ulpiani, Water mist spray for outdoor cooling: A systematic review of technologies, methods and impacts, *Appl. Energy* 254 (2019) 113647.
- [8] S. Alvarez, E. Rodriguez, J. Molina, The Avenue of Europe at Expo 92: Application of cool towers, in: *Architecture and Urban Space: 9th PLEA International Conference*, Seville, Spain, 1991, pp. 195–201.
- [9] R. Magrou, Theatre to the world. The transformation of the Place de la République, Paris, *Topos: Eur. Landsc. Mag.* (91) (2015) 62.
- [10] A. Fernandez Per, J. Arpa, the Public Chance – New Urban Landscapes, a+ architecture publishers, 2008, p. 420.
- [11] W. Oh, R. Ooka, J. Nakano, H. Kikumoto, O. Ogawa, Environmental index for evaluating thermal sensations in a mist spraying environment, *Build. Environ.* 161 (2019) 106219.
- [12] M. Zhang, C. Xu, L. Meng, X. Meng, Outdoor comfort level improvement in the traffic waiting areas by using a mist spray system: An experiment and questionnaire study, *Sustainable Cities Soc.* 71 (2021) 102973.
- [13] D. Narumi, K. Shigematsu, Y. Shimoda, Effect of the evaporative cooling techniques by spraying mist water on reducing urban heat flux and saving energy in apartment house, in: *2nd Int. Conf. Countermeas.*, 2009.
- [14] N. Wong, A.Z. Chong, Performance evaluation of misting fans in hot and humid climate, *Build. Environ.* 45 (12) (2010) 2666–2678.
- [15] C. Huang, D. Ye, H. Zhao, T. Liang, Z. Lin, H. Yin, Y. Yang, The research and application of spray cooling technology in Shanghai ?expo, *Appl. Therm. Eng.* 31 (17–18) (2011) 3726–3735.
- [16] C. Huang, J. Cai, Z. Lin, Q. Zhang, Y. Cui, Solving model of temperature and humidity profiles in spray cooling zone, *Build. Environ.* 123 (2017) 189–199.
- [17] C. Farnham, K. Emura, T. Mizuno, Evaluation of cooling effects: outdoor water mist fan, *Build. Res. Inform.* 43 (3) (2015) 334–345.
- [18] H. Esen, O. Tuna, Investigation of photovoltaic assisted misting system application for arbor refreshment, *Int. J. Photoenergy* 2015 (2015).
- [19] K. Zheng, M. Ichinose, N.H. Wong, Parametric study on the cooling effects from dry mists in a controlled environment, *Build. Environ.* 141 (2018) 61–70.
- [20] G. Ulpiani, E. Di Giuseppe, C. Di Perna, M. D'Orazio, M. Zinzi, Thermal comfort improvement in urban spaces with water spray systems: Field measurements and survey, *Build. Environ.* 156 (2019) 46–61.
- [21] G. Ulpiani, C. di Perna, M. Zinzi, Water nebulization to counteract urban overheating: Development and experimental test of a smart logic to maximize energy efficiency and outdoor environmental quality, *Appl. Energy* 239 (2019) 1091–1113.
- [22] G. Ulpiani, C. di Perna, M. Zinzi, Mist cooling in urban spaces: Understanding the key factors behind the mitigation potential, *Appl. Therm. Eng.* 178 (2020) 115644.
- [23] A. Desert, E. Naboni, D. Garcia, The spatial comfort and thermal delight of outdoor misting installations in hot and humid extreme environments, *Energy Build.* 224 (2020) 110202.
- [24] W. Oh, R. Ooka, J. Nakano, H. Kikumoto, O. Ogawa, Evaluation of mist-spraying environment on thermal sensations, thermal environment, and skin temperature under different operation modes, *Build. Environ.* 168 (2020) 106484.
- [25] J. Kim, J. Kang, Evaluating the efficiency of fog cooling for climate change adaptation in vulnerable groups: A case study of Daegu Metropolitan City, *Build. Environ.* 217 (2022) 109120, <http://dx.doi.org/10.1016/j.buildenv.2022.109120>, URL <https://www.sciencedirect.com/science/article/pii/S0360132322003572>.
- [26] M. Su, B. Hong, X. Su, A. Liu, J. Chang, How the nozzle density and height of mist spraying affect pedestrian outdoor thermal comfort: A field study, *Build. Environ.* 215 (2022) 108968, <http://dx.doi.org/10.1016/j.buildenv.2022.108968>, URL <https://www.sciencedirect.com/science/article/pii/S0360132322002104>.
- [27] A.P. Gagge, An effective temperature scale based on a simple model of human physiological regulatory response, *AHSRAE Trans.* 77 (1971) 247–262.
- [28] P. Höppe, The physiological equivalent temperature—a universal index for the biometeorological assessment of the thermal environment, *Int. J. Biometeorol.* 43 (2) (1999) 71–75.
- [29] C. Yaglou, D. Minaed, et al., Control of heat casualties at military training centers, *Arch. Indust. Health* 16 (4) (1957) 302–316.
- [30] G. Jendritzky, R. de Dear, G. Havenith, UTCI – Why another thermal index? *Int. J. Biometeorol.* 56 (3) (2012) 421–428.
- [31] A.P. Gagge, Y. Nishi, Heat exchange between human skin surface and thermal environment, *Comprehen. Physiol.* (2010) 69–92.
- [32] W. Oh, R. Ooka, J. Nakano, H. Kikumoto, O. Ogawa, Extended standard effective temperature index for water-misting environment, *Build. Environ.* 190 (2021) 107573.
- [33] W. Oh, R. Ooka, J. Nakano, H. Kikumoto, O. Ogawa, W. Choi, Development of physiological human model considering mist wettedness for mist-spraying environments, *Build. Environ.* 180 (2020) 106706.
- [34] W. Köppen, R. Geiger, *Handbuch Der Klimatologie*, vol. 1, Gebrüder Borntraeger Berlin, 1930.
- [35] S. Falasca, G. Curci, F. Salata, On the association between high outdoor thermo-hygrometric comfort index and severe ground-level ozone: A first investigation, *Environ. Res.* 195 (2021) 110306.
- [36] American Society of Heating, Refrigerating and Air-Conditioning Engineers, *ASHRAE Standard* 55, 2020.
- [37] P.O. Fanger, *Thermal Comfort. Analysis and Applications in Environmental Engineering*, Danish Technical Press., Copenhagen, 1970, p. 244.
- [38] H. Montazeri, B. Blocken, J.L. Hensen, CFD analysis of the impact of physical parameters on evaporative cooling by a mist spray system, *Appl. Therm. Eng.* 75 (2015) 608–622.
- [39] H. Montazeri, B. Blocken, J. Hensen, Evaporative cooling by water spray systems: CFD simulation, experimental validation and sensitivity analysis, *Build. Environ.* 83 (2015) 129–141.